J Solid State Electrochem (2011) 15:703–709
DOI 10.1007/s10008-010-1140-7

ORIGINAL PAPER

EIS study on the corrosion performance of a Cr(III)-based conversion coating on zinc galvanized steel for the automotive industry

Francesco Rosalbino · Giorgio Scavino · Giovanni Mortarino · Emma Angelini · Giancarlo Lunazzi

Received: 16 March 2010 / Revised: 30 June 2010 / Accepted: 3 July 2010 / Published online: 21 July 2010

Abstract The corrosion performance of a new industrial Cr (III)-based conversion coating on zinc galvanized FeP04 steel for the automotive industry was studied. For comparison, the zinc galvanized steel submitted to a Cr(VI)-based passivation treatment was also examined. The corrosion behavior was assessed by means of potentiodynamic polarization and electrochemical impedance spectroscopy measurements in aerated 0.1 M NaCl solution. The behavior of untreated zinc galvanized FeP04 steel in aerated 0.1 M NaCl solution was also studied. The results obtained indicate that with the same thickness, the coating generated in the Cr(III) treatment bath exhibits better corrosion properties compared to the coating formed in the Cr(VI) treatment bath. The difference in the corrosion protection given by the two conversion coating types can be ascribed to the difference in the chromium content and coating composition.

Keywords Zinc galvanized FeP04 steel · Cr(III)-based conversion coating · Chromates · Electrochemical impedance spectroscopy (EIS) · Passivation

F. Rosalbino (✉) · G. Scavino · G. Mortarino · E. Angelini
Dipartimento di Scienza dei Materiali ed Ingegneria Chimica,
Politecnico di Torino,
Turin, Italy
e-mail: francesco.rosalbino@polito.it

G. Lunazzi
FIAT Auto S.p.A., Torino,
Turin, Italy

Introduction

The automotive industry requires protective coatings with high degradation resistance. The coating must protect the substrate against corrosive attack and maintain, for a long time, good aesthetic properties [1]. Among the metallic coatings used to protect steel surfaces in the automotive industry, galvanized zinc coatings are widely used since they behave as barrier layers to inhibit the carbon steel from oxidation by outdoor exposure. Zinc coatings also provide galvanic protection, as sacrificial anodes, for exposed areas of the steel substrates [2, 3]. The corrosion resistance qualities of zinc coatings are improved by means of chemical surface treatments and organic coatings. After application of the zinc coatings on steels, the chromate conversion coatings (CCCs) are subsequently deposited to provide the visual color and perform an effective protection from corrosion. However, Cr(IV) compounds are classified as carcinogen due to their intrinsic toxicity [4–6], and government legislation has limited their usage [7, 8] by the RoHS directives from the European Union since 2006.

Many different conversion coatings have been studied as possible alternatives to traditional CCCs in addition to the typical phosphating treatment: chromium-free, including molybdates, permanganates, vanadates and tungstates (conversion coatings with protecting mechanism similar to CCCs acting as passivating agents) [9, 10], or adhesion promoters like fluo-zirconates, fluo-titanates, organosilanes, etc. [11, 12].

A further possibility is to use conversion coatings based on Cr(III), which is not considered carcinogenic [13].

Several papers are available in the literature dealing with Cr(III)-based conversion coatings deposited on zinc galva-

nized steel surfaces and their corrosion protection characterization [14–16]. However, the main results are scattered and are not clear in terms of practical applications. As is well known, the study of the corrosion performance of zinc conversion coatings allows important conclusions to be drawn regarding the application of the technology. Usually, the most important tests for this specific application were as follows: neutral saline cabinet [17], humidity cabinet [18], Kesternich test [19], sodium chloride–acetic acid test [20], synthetic seawater test and the field exposure tests. Unfortunately, the results of the above tests are sometimes ambiguous for laboratory tests, and the field exposure tests are very efficient but time-consuming.

Electrochemical methods, in particular electrochemical impedance spectroscopy (EIS) technique, have been shown in numerous studies to be an efficient and convincing tool for analyzing the corrosion performance of both organic and inorganic coatings [21].

In this work, the EIS technique has been used to study the corrosion performance of a new industrial Cr(III)-based conversion coating on zinc galvanized steel for the automotive industry upon exposure to a 0.1 M NaCl aqueous solution. Morphological investigations have been performed on the coating surface by scanning electron microscopy (SEM) before and after the electrochemical tests.

Experimental

Zinc coatings were obtained on FeP04 steel sheets employed in the automotive industry, whose composition is reported in Table 1.

The coatings were produced in an industrial rack plant from a cyanide-free alkaline bath reported in Table 2. The coating thickness was about 10±1 μm.

After zinc deposition, the samples were submitted to conversion treatments in two industrial baths. The first bath is a traditional chromate treatment based on Cr(VI), working temperature 25 °C, with 2 g l^{-1} Cr(VI), pH 1.8; the time of permanence in the bath is 30 s (conversion treatment symbol Cr(VI)). The second conversion treatment is based on Cr(III), working temperature 60 °C, with 10 g l^{-1} Cr(III), pH 2.0; this solution contains Co(II) ions (5 g l^{-1} Co(II)) in addition to Cr(III); the time of permanence in the bath is 60 s (conversion treatment symbol Cr(III)). The chromium content of the conversion coatings was determined by means of inductively coupled plasma spectroscopy after stripping the deposits in HCl 1:3 with hexamethylenetetramine to inhibit dissolution of the steel substrate.

Table 1 Chemical composition (wt.%) of the FeP04 steel

C	Mn	Si	Ni	P	S	Al	Ti
0.003	0.1	0.03	0.003	0.002	0.007	0.03	0.06

Table 2 Composition of the bath for the electrodeposition of zinc coatings

Bath	Composition (gl^{-1})	Temperature (°C)	Current density (Adm^{-2})
Zn alkaline	Zn 10–20; NaOH 80–100; Additives	20–35	1.5–3

Before and after the electrochemical tests, morphological analysis of the coatings was performed by means of SEM. To evaluate the conversion coating thickness, the sample was fractured in liquid N_2 and SEM analysis was carried out on the cross-sections.

The protective properties of the conversion coatings were studied by means of potentiodynamic polarization and EIS measurements.

Potentiodynamic polarization measurements were carried out in a glass cell containing a treated or untreated zinc-coated steel sample, a platinum counter electrode and a saturated calomel reference electrode (SCE) connected to the cell with a lugging capillary. Measurements were performed in aerated 0.1 M NaCl aqueous solution (pH 6) at room temperature. Polarization curves were recorded at a scan rate of 1 mV s^{-1} after allowing a steady-state potential to develop. IR drop compensation was achieved using current interruption method. The surface area exposed to the test solution was 12 cm^2.

EIS measurements were carried out on untreated, Cr (VI)- and Cr(III)-treated zinc-coated steel samples in the aerated 0.1 M NaCl solution at room temperature. The counter electrode was a concentric piece of flat platinum net that was parallel to the surface of the steel sample. The reference electrode was a saturated calomel reference electrode. The frequency range analyzed went from 10 kHz up to 10 MHz for the untreated and from 100 kHz to 10 MHz for the Cr(VI)- and Cr(III)-treated zinc-coated steel samples, with the frequency values spaced logarithmically (seven per decade). The width of the sinusoidal voltage signal applied to the system was 10 mV root mean square. The surface area exposed to the test solution was 12 cm^2. Impedance measurements were performed in the potentiostatic mode at the open circuit potential as a function of exposure time to the aggressive environment. Measurements were carried out in triplicate, and the average values are reported. All the impedance data were modeled and interpreted using the Equivcrt software fitting procedure developed by Boukamp [22].

Results and discussion

Surface characterization

The chemical–physical characteristics (thickness and chromium content) of the Cr(VI)- and Cr(III)-based conversion coatings are reported in Table 3. These data indicate that even though the treatment time and temperature are different, the conversion coating grows to the same thickness both in the Cr(VI) and in the Cr(III) treatment solution. However, the coating generated in the Cr(III) treatment bath exhibits a higher Cr content.

Figure 1 shows the surface morphology of zinc-coated FeP04 steel sheets submitted to Cr(VI)-based (Fig. 1a) and Cr(III)-based (Fig. 1b) conversion treatments. In both cases, the surface is rough and no microcracks are present, but preferentially etched zones are visible, suggesting that the formation of the coating is influenced by the orientation of individual zinc grains.

Two parallel processes were proposed for the Cr(III)-based conversion coatings: dissolution of zinc with simultaneous evolution of hydrogen [23, 24]:

$$\text{Anodic reaction}: Zn \rightarrow Zn^{2+} + 2e^{-} \quad (1)$$

$$\text{Cathodic reaction}: 2H^{+} + 2e^{-} \rightarrow H_2 \quad (2)$$

The reduction of hydrogen ions leads to an increase of pH value in the vicinity of the Zn surface, which results in the precipitation of chromium oxide/hydroxide and zinc hydroxide from Cr(III) and Zn(II) ions:

$$Zn^{2+} + 2OH^{-} \rightarrow Zn(OH)_2 \quad (3)$$

$$Cr^{3+} + 3OH^{-} \rightarrow Cr(OH)_3 \quad (4)$$

$$2Cr^{3+} + 6OH^{-} \rightarrow Cr_2O_3 + 3H_2O \quad (5)$$

X-ray photoelectron spectroscopy (XPS) analysis of the Cr(III)-based conversion coating (Rosalbino et al., accepted for publication) revealed the presence of zinc oxides/hydroxides, cobalt oxides/hydroxides, as well as chromium oxides/hydroxides. About 40% of the chromium in the coating is in the form of $Cr(OH)_3$, while about 60% is in the form of Cr_2O_3. For the Cr(VI)-based conversion coating, XPS analysis (Rosalbino et al., accepted for publication) revealed that about 40% of the total Cr is in the Cr(VI) oxidation state. About 30% of the Cr is in the form of $Cr(OH)_3$ and 30% is in the form of Cr_2O_3.

Table 3 Chemical–physical characteristics of the conversion coatings

Conversion treatment	Thickness (μm)	Cr content (μg cm^{-2})
Cr (VI)	0.30±0.01	12±1
Cr (III)	0.30±0.01	20±1

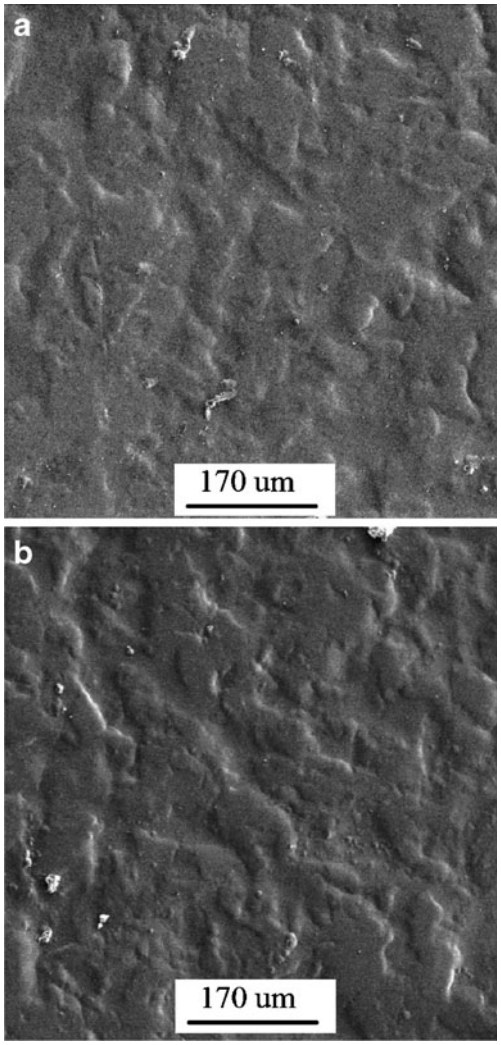

Fig. 1 Surface morphology (SEM-BSE) of the zinc-coated FeP04 steel sheets submitted to conversion treatments: **a** Cr(VI)-based conversion coating; **b** Cr(III)-based conversion coating

Electrochemical characterization

Polarization measurements

Figure 2 reports the potentiodynamic polarization curves for untreated, Cr(VI)- and Cr(III)-treated zinc-coated FeP04 steel specimens in aerated 0.1 M NaCl solution. As can be seen, the anodic polarization curves for the untreated and treated surfaces are all quite similar. The cathodic polarization curves, however, are significantly different. The

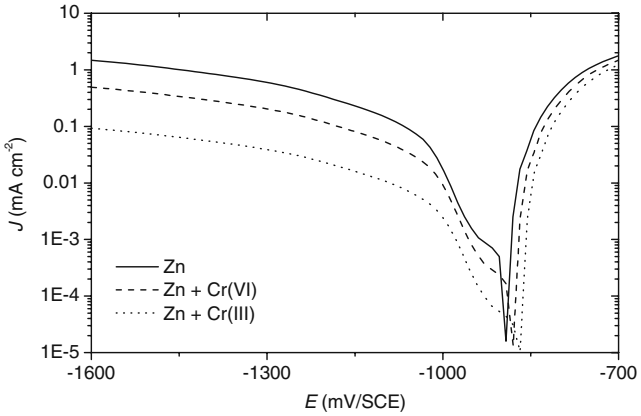

Fig. 2 Potentiodynamic polarization curves for untreated, Cr(VI)- and Cr(III)-treated zinc coated FeP04 steel in aerated 0.1 M NaCl solution

zinc-coated FeP04 steel specimen show the largest cathodic current density, while the Cr(III)-treated specimen exhibits the smallest current density.

In near-neutral aerated solutions containing Cl^- anions, the corrosion of zinc is controlled by oxygen diffusion according to the following half-reactions [25–27]:

$$Zn \rightarrow Zn^{2+} + 2e^- \quad (6)$$

$$O_2 + 4H^+ + 4e^- \rightarrow 2H_2O \quad (7)$$

The polarization curves reported in Fig. 2 show that Cr(VI) and Cr(III) treatments can both reduce the cathodic current density, forming an effective barrier layer: They can hinder the transport of oxygen to the zinc substrate and consequently retard the corrosion of zinc. Nevertheless, the results obtained suggest that the inhibition of the corrosion of zinc provided by the Cr(III)-based conversion coating is more effective than the inhibition by the Cr(VI)-based conversion coating. As a matter of fact, the cathodic reaction rate for the Cr(III)-treated zinc-coated FeP04 steel is significantly lower than that for Cr(VI)-treated zinc-coated FeP04 steel (Fig. 2).

Impedance measurements

Figure 3 shows Bode impedance plots for zinc-coated FeP04 steel sheets untreated (Fig. 3a) and submitted to Cr (VI)-based (Fig. 3b) and Cr(III)-based (Fig. 3c) conversion treatments, obtained as a function of the exposure time to aerated 0.1 M NaCl solution.

In the case of untreated specimens, the characteristic shape of Bode diagrams suggests that the corrosion of zinc-coated FeP04 steel is a charge transfer-controlled dissolution reaction [26, 27]. The impedance data were fitted with a simple equivalent circuit (Fig. 4a). In this equivalent circuit, R_s represents the electrolyte resistance, C_{dl} represents the double-layer capacitance and R_{ct} represents the charge transfer of the electrode reactions. A constant phase element, CPE, (Q_{dl}), is used to represent the non-ideal capacitive response of the system. The impedance of a CPE is given by the equation: $Z_{CPE} = Y_0{}^{-1}(j\omega)^{-n}$, where Y_0 is the admittance constant of the CPE (in $s^n\ \Omega^{-1}\ cm^{-2}$), ω is the angular frequency (rad s^{-1}) and n is the CPE exponent, $n = \alpha/(\pi/2)$ (α is the constant phase angle of the CPE) [28]. According to the fitting results, the n values are >0.9, indicating that $Q_{dl} \approx C_{dl}$. A very good agreement between experimental and theoretical data was obtained. A standard deviation χ-quadrate was in the order of 10^{-5} (the smaller this value is, the closer the fit is to the experimental data), and the relative error was <5%.

The response of Cr(VI)- and Cr(III)-treated samples to an applied potential perturbation was modeled with the equivalent circuit reported in Fig. 4b, where R_{Cr} and C_{Cr} represent the resistance and capacitance of the chemical conversion coating, respectively. Thus, the capacitive response of the conversion coating determines the behavior of the system at high frequencies, whereas the capacitive response of the double layer determines the behavior at lower frequencies [29, 30]. Both the time constants exhibit some Cole–Cole type dispersion which has the corresponding n_i parameter, being $0<n_i\leq 1$. Furthermore, distortions observed in the resistive–capacitive contributions indicate a deviation from the theoretical model in terms of a time-constant distribution due to either lateral penetration of the electrolyte at the metal/coating interface or underlying metallic surface heterogeneity (topological, chemical composition, surface energy): Since all these factors cause the impedance/frequency relationship to be nonlinear, they are taken in consideration by replacing the capacitive components (C_{dl}, C_{Cr}) of the equivalent circuit (Fig. 4b) by the corresponding constant phase element, CPE, (Q_{dl}, Q_{Cr}). According to the fitting results, the n_i values are >0.9, indicating that $Q_{dl} \approx C_{dl}$ and $Q_{Cr} \approx C_{Cr}$. A very good agreement between experimental and theoretical data was obtained. A standard deviation χ-quadrate was in the order of 10^{-5}, and the relative error was <5%.

The more interesting data to discuss are the resistance of the conversion coating, R_{Cr}, giving information on the barrier properties of the chemical conversion layer and the charge transfer resistance, R_{ct}, giving information on the kinetics of the corrosive process.

Evolution of the resistance of the chemical conversion coating, R_{Cr}, as a function of exposure time to aerated 0.1 M NaCl solution is reported in Fig. 5. The Cr(III)-based conversion coating appears to offer better barrier properties in comparison with the Cr(VI)-based conversion layer. This fact has a strong influence on the charge transfer resistance and therefore on the corrosion rate, as can be seen in Fig. 6. The sample submitted to Cr(III)-based conversion treatment

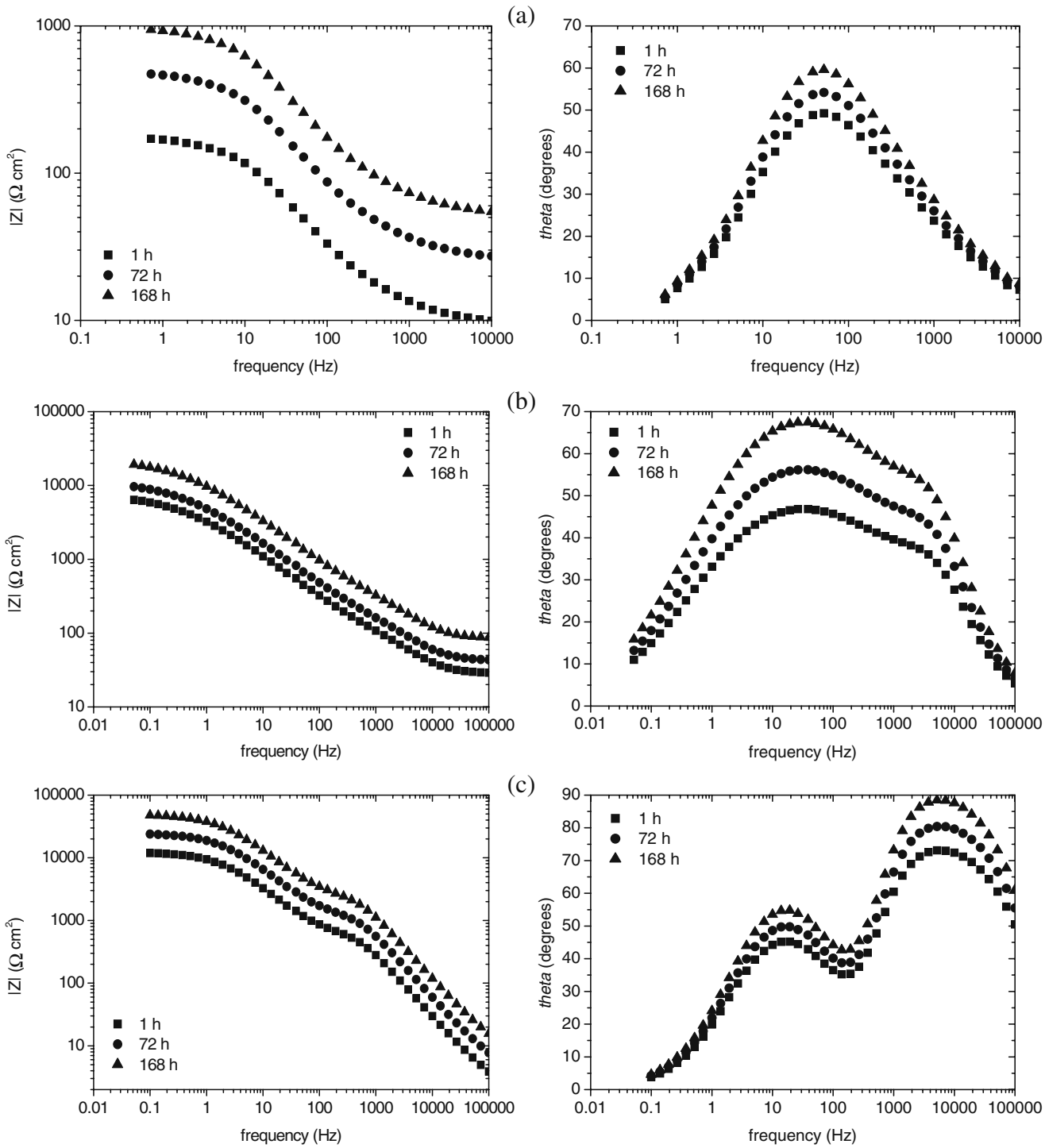

Fig. 3 Bode impedance plots as a function of exposure time obtained in aerated 0.1 M NaCl solution for: untreated (**a**); Cr(VI)-treated (**b**); and Cr (III)-treated zinc coated FeP04 steel (**c**)

shows higher R_{ct} values and therefore lower corrosion rate. In Fig. 6, it is possible to note an increase of the R_{ct} values, increasing the exposure time to the aggressive solution. This phenomenon can be attributed to the passivation properties of the conversion layer for Cr(VI)- and Cr(III)-treated samples or to the accumulation of zinc corrosion products acting partially as a barrier for the zinc-coated FeP04 steel [30, 32]. SEM characterization of the specimen surface at the end of EIS measurements (Fig. 7) confirmed the presence of corrosion products, which, by X-ray diffraction, were found to be ZnO and $ZnCl_2{\cdot}4Zn(OH)_2$ (Rosalbino et al., accepted for publication). On the other

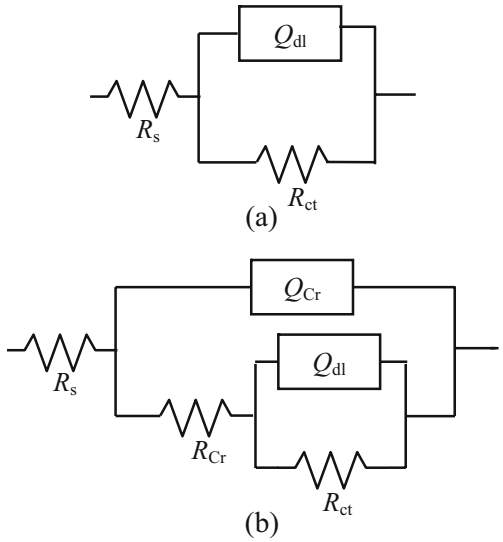

Fig. 4 Equivalent circuits used to model: untreated zinc coated FeP04 steel (**a**) and Cr(VI)- and Cr(III)-treated zinc-coated FeP04 steel in aerated 0.1 M NaCl solution (**b**)

hand, increasing exposure time to the aggressive environment, a decrease of the double-layer capacitance is observed (C_{dl} ranges between 105 and 30 × 10^{-5} F cm^{-2} for the Cr(VI)-based conversion coating and between 80 and 0.5 × 10^{-5} F cm^{-2} for the Cr(III)-based conversion coating), indicating a surface passivation [9, 30].

The high C_{dl} values obtained for short exposure times (<24 h) to the aggressive environment can be associated to localized corrosion phenomena occurring at the electrolyte/metal interface due to intrinsic coating defects (pores or pinholes) [29, 32]. The double-layer capacitance is proportional to the area involved in the electrochemical reaction, i.e. surface area of pores or pinholes in contact with the aggressive environment. Therefore, the decrease of C_{dl} indicates that the corrosion inside the intrinsic coating defects becomes less severe and the surface area of the pores or pinholes decreases with increasing exposure time due to the passivation process.

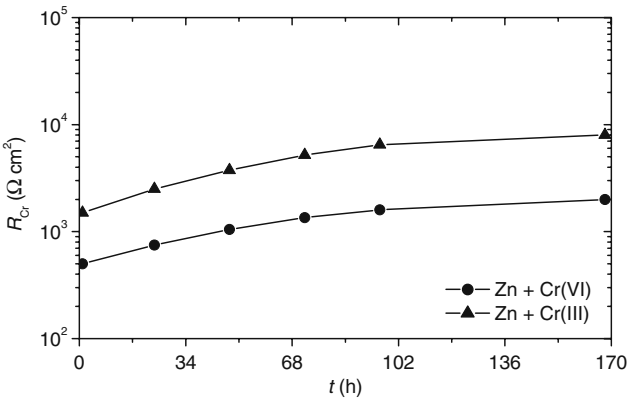

Fig. 5 Variation of the chemical conversion layer resistance, R_{Cr}, as a function of exposure time to aerated 0.1 M NaCl solution

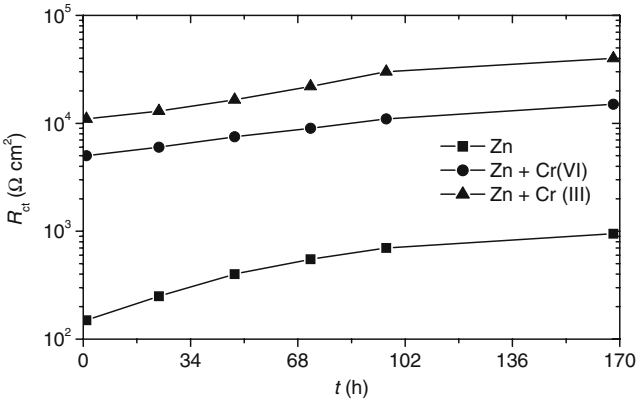

Fig. 6 Variation of the charge transfer resistance, R_{ct}, as a function of exposure time to aerated 0.1 M NaCl solution

Further discussion

The better corrosion properties exhibited by the conversion coating based on Cr(III) compared to the Cr(VI)-based conversion coating, with the same thickness, may be attributed to the higher chromium content and to the difference in the coating composition. When a conversion layer is used as the outermost one in the coating system, electrochemical interactions between this layer and its surrounding medium start after getting in contact, particularly if the medium is a saline aqueous solution. In such circumstances, both the chromium content and the insoluble components ($Cr(OH)_3$ and Cr_2O_3) of the conversion layer play a decisive role,

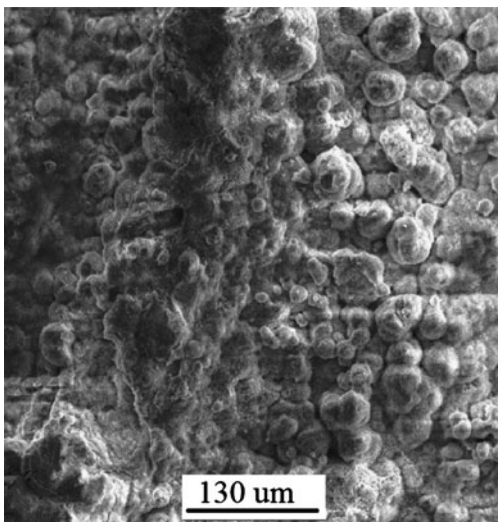

Fig. 7 SEM-BSE micrograph of the corrosion products layer formed at the surface of zinc-coated FeP04 steel after 168-h exposure to aerated 0.1 M NaCl solution

either providing a barrier resistance to the corrosion-inducing species diffusion towards the underlying zinc or inhibiting the oxygen reduction reaction [33–35]. In both types of conversion coating, the chromium is mainly in the Cr(III) oxidation state. However, the coating generated in the Cr(III) treatment bath exhibits higher $Cr(OH)_3$ and Cr_2O_3 amounts with respect to the coating generated in the Cr(VI) treatment bath. Moreover, coatings generated in a Cr(III) treatment bath containing transition metal ions such as Co(II), Ni(II) and Fe (II) showed superior corrosion resistance than that formed in the bath without transition metal ions [31, 32, 36]. Thus, the increased corrosion resistance of the Cr(III)-treated zinc-coated FeP04 steel sample with respect to the Cr(VI)-treated one may be ascribed to improved protective properties of the Cr(III)-based conversion layer which acts as an effective physical barrier against corrosion progress.

Further investigation is planned aiming at a deeper understanding of the corrosion properties of the Cr(III)-based conversion coating.

Conclusions

The corrosion performance of a new industrial Cr(III)-based conversion coating on zinc galvanized FeP04 steel for the automotive industry was studied in aerated 0.1 M NaCl solution by potentiodynamic polarization and electrochemical impedance spectroscopy measurements. For comparison, the zinc galvanized steel submitted to a Cr(VI)-based passivation treatment was also examined.

Coatings generated in Cr(VI) and Cr(III) treatments baths can inhibit corrosion in near-neutral aerated solutions containing Cl^- anions by hindering the transport of oxygen to the zinc substrate, thereby retarding the cathodic half-reaction. However, the results obtained in this study indicate that with the same thickness, the inhibition of the corrosion of zinc galvanized FeP04 steel provided by the Cr(III)-based conversion coating appears more effective than the inhibition provided by the Cr(VI)-based conversion coating.

The different corrosion protection of the two types of conversion coating is attributed to the difference in the chromium content and coating composition. Owing to the higher chromium and chromium(III) oxide/hydroxide amounts, the coating formed in the Cr(III) treatment bath exhibits enhanced barrier properties compared to the Cr (VI)-based conversion coating.

References

1. Bauer DR (1994) J Coat Technol 66:57
2. Graedel TE (1989) J Electrochem Soc 136:193
3. Nevison DCH (1987) ASM handbook. ASM International, Materials Park, p 755
4. Wilcox GD, Warthon JA (1997) Trans IMF 75:B140
5. Jeffcoate CS, Isaacs HS, Aldykiewicz AJ, Ryan MP (2000) J Electrochem Soc 147:540
6. Hagans PL (1994) ASM handbook. ASM International, Materials Park, p 405
7. Wynn PC, Bishop CV (2001) Trans Inst Met Finish 79:B27
8. Wilcox GD (2003) Trans Inst Met Finish 81:B13
9. Almeida E, Fedrizzi L, Diamantino TC (1998) Surf Coat Technol 105:97
10. Almeida E, Diamantino TC, Figueiredo MO, Sà C (1998) Surf Coat Technol 106:8
11. Puomi P, Fagerholm HM, Rosenholm JB, Jyrka K (1999) Surf Coat Technol 115:79
12. Yuan W, Van Ooji W (1997) J Colloid Interface Sci 185:197
13. Bellezze T, Roventi G, Fratesi R (2002) Surf Coat Technol 155:221
14. Lionel T (2000) Galvanotechnik 91:3373
15. Gardner A, Scharf J (2001) Soc Automot Eng SP-1614, p 95
16. Zaki N (2002) Met Finish 100:492
17. ASTM-B-117 (1990) Salt spray (fog) testing. ASTM, Philadelphia
18. DIN 50117 (1982) Atmospheres and their technical application condensation water test atmospheres. DIN, Berlin
19. DIN 50118 (1982) Testing in a saturated atmosphere in the presence of sulphur dioxide. DIN, Berlin
20. ISO/DIS 9227.2 (1989) Essai de Corrosion en Atmosphères Artificielles–Essai aux Brouillards Salins. ISO, Geneva
21. De Wit JHW (1995) Corrosion mechanisms in theory and practice. Marcel Dekker, New York, p 581
22. Boukamp B (1986) Solid State Ionics 20:31
23. Magalhaes AAO, Tribollet B, Mattos OR, Margarit ICP, Barcia OE (2003) J Electrochem Soc 150:B16
24. Martyak NM (1996) Surf Coat Technol 88:139
25. Baugh LM (1979) Electrochim Acta 24:657
26. Fedrizzi L, Ciaghi L, Bonora PL, Fratesi R, Roventi G (1992) J Appl Electrochem 22:247
27. Zhang XG (1996) Corrosion and electrochemistry of zinc. Plenum, New York
28. Macdonald JR (1987) Impedance spectroscopy. Wiley, New York
29. Zhang X, Van Den Bos C, Sloof WG, Hovestad A, Terryn H, De Wit JHW (2005) Surf Coat Technol 199:92
30. Deflorian F, Rossi S, Fedrizzi L, Bonora PL (2006) Prog Org Coat 52:271
31. Da Fonte B, Mich MC (1982) US Patent 4,359,345
32. Choo KW, Rao VS, Kwon HS (2007) Electrochim Acta 52:4449
33. Biestek T, Weber J (1976) Conversion coatings. Portcullis, Redhill
34. Kendig M, Addison R, Jeanjaquet S (1999) J Electrochem Soc 146:4419
35. Xia L, Akiyama E, Frankel G, Mc Creery R (2000) J Electrochem Soc 147:2556
36. Fratesi R, Roventi G, Tomachuk CR (1997) J Appl Electrochem 27:1088